

FLAME SPREAD IN A MICROGRAVITY ENVIRONMENT- ROLE OF FUEL THICKNESS

SUBRATA BHATTACHARJEE
San Diego State University, San Diego, California

and

KAZUNORI WAKAI
SHUHEI TAKAHASHI
Gifu University, Gifu, Japan

INTRODUCTION: Fueled by a necessity to develop an understanding of flame spread in microgravity environment due to the fire safety aspects in manned spacecrafts, considerable work has been done during the last decade [1] on laminar flame spread over solid fuels. In this study, we present a simplified scale analysis and recently acquired spread rate data in the MGLAB, Japan [2] to address the role played by fuel thickness in opposed-flow flame spread with emphasis on the limiting case of the quiescent environment.

LENGTH AND TIME SCALES: To describe the heat-transfer limited mechanism, we focus our attention in Fig. 1 at the leading edge of the flame where the forward heat transfer[3] occurs. With respect to the flame the oxidizer approaches the flame with a velocity $V_r = V_g + V_f$ (V_g can be due to forced or buoyancy induced) and the fuel with a velocity V_f . Two control volumes, one in the gas phase of size $L_{gx} \times L_{gy} \times W$ and one in the solid phase of size $L_{sx} \times L_{sy} \times W$, are shown, W being the fuel-width in the z direction and the length scales, L_{gx} , L_{gy} , L_{sx} and L_{sy} , unknown at this point.

There are two characteristic resident times at the leading edge, $t_{res,g} \sim L_{gx} / V_r$ in the gas phase and $t_{res,s} \sim L_{sx} / V_f$ in the solid.

In the gas-phase, a balance between the conduction and convection in the x -direction at the leading edge yields the familiar[3] expression for L_{gx} , while L_{gy} can be obtained following Delichatsios[4] as the diffusion length in the y -direction within the available residence time. .

$$L_{gx} \sim \frac{\alpha_g}{V_r} \quad L_{gy} \sim \sqrt{\alpha_g t_{res,g}} = \frac{\alpha_g}{V_r} = L_{gx} \quad L_g \equiv L_{gx} = L_{gy} \quad (1).$$

The gas-phase conduction being the driving force under all but extreme situations [5], L_g is imposed on the solid phase making $L_{sx} \sim L_g$. The transverse length L_{sy} , derived in a manner similar to L_{gy} , however, cannot be greater than the half-thickness of the fuel. Therefore,

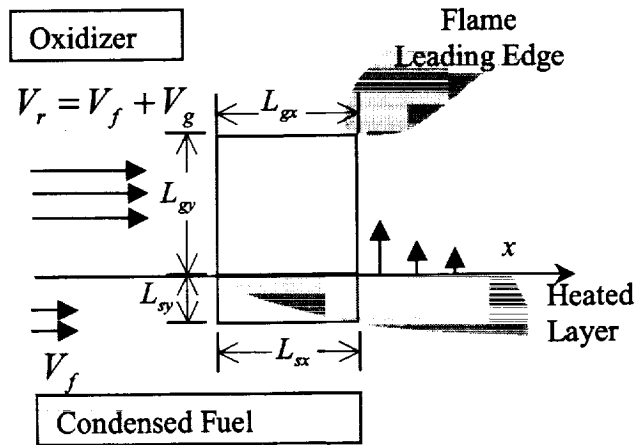


Fig. 1 Control volumes at the flame leading edge in the gas and the solid phases.

$$L_{sx} \sim L_g = \frac{\alpha_g}{V_r} \quad \text{and, } L_{sy} \sim \min \left[\tau, \sqrt{\alpha_s \frac{L_{sx}}{V_f}} \right] = \min \left[\tau, \sqrt{\frac{\alpha_s \alpha_g}{V_f V_r}} \right]. \quad (2).$$

THERMAL REGIME: In thermal regime $t_{res,g}$ is assumed large compared to the characteristic chemical time t_{comb} justifying the assumption of infinitely fast chemistry and small compared to the radiative time scales justifying the neglect of all radiative effects. of flame spread is based on a few simplifying assumptions. The characteristic vaporization time t_{vap} is assumed small compared to $t_{res,s}$ allowing the use of a constant vaporization temperature. An energy balance for the solid phase control volume yields the spread rate.

$$\lambda_g \frac{(T_f - T_v)}{L_{gy}} L_{gx} W \sim V_f \rho_s c_s L_{sy} W (T_v - T_{F,\infty}) \quad (3).$$

Hence, $V_f \sim \frac{\lambda_g}{\rho_s c_s L_{sy}} F$ where, $F \equiv \frac{T_f - T_v}{T_v - T_{F,\infty}}$ (4).

Substituting L_{sy} from Eq. (2) produces the familiar[6] thin and the thick limits.

$$V_{f,thin} \sim \frac{\lambda_g}{\rho_s c_s \tau} F \quad \text{and} \quad V_{f,thick} \sim V_r \frac{\lambda_g \rho_g c_g}{\lambda_s \rho_s c_s} F^2 \quad (5a,5b)$$

In order to reduce the errors in Eq. (5) resulting from the simplifying assumptions, Bhattacharjee et. al[5] proposed a simplified theory (EST) , which replaced V_g with an equivalent velocity taking into account the boundary layer development, introduced a flame temperature correction and prescribed T_v as the appropriate temperature for property evaluation.

THICK VS. THIN FUELS: Equating the two limiting cases [Eqs. 5a and 5b], we obtain the scale for the transition thickness.

$$\tau_{cr,thin-thick} \sim \frac{\lambda_s L_g}{\lambda_g F}. \quad (6)$$

In non-dimensional terms, Eqs. 5(a) and 5(b) can be combined.

$$\eta \equiv \frac{V_f}{V_{f,thick,EST}} = \min \left(1, \frac{1}{T} \right) \quad \text{where, } T \equiv \tau / \tau_{cr,thin-thick,EST} \quad (7).$$

Computational results suggest that the fuel becomes thermally thick for $T \geq 2$, a conclusion that has been found to be independent of flow configuration. The recent data [7] for downward spread where the fuel thickness has been varied over a wide range is reproduced in Fig. 2. Although the spread rate is somewhat overpredicted by Eq. (7), the transition seems to be around $T \geq 2$ even though significant

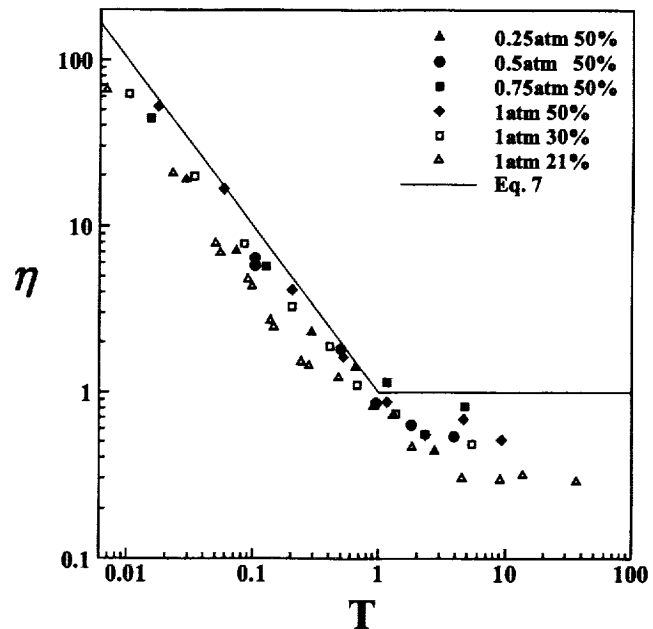


Fig. 2 Downward spread rate data over PMMA for different fuel thicknesses and ambient conditions.

kinetic effects are present. Unfortunately, there is no forced opposed-flow experiment in which the thickness of a fuel has been varied from the thin to the thick limit in the thermal regime.

QUIESCENT ENVIRONMENT: In the absence of forced or induced motion V_r (see Fig. 1) must be replaced with V_f . By substituting $V_{f,thin}$ from Eq. (5), an upper limit for V_f in Eq. (2), it can be shown that

$$L_{sy} \sim \min[\tau, \tau_0] = \tau \quad \text{because, } \tau_0 = \sqrt{\frac{\alpha_s \alpha_g}{V_f V_r}} > \sqrt{\frac{\alpha_s \alpha_g}{V_{f,Thin} V_r}} = \tau F \sqrt{\frac{\lambda_s \rho_s c_s}{\lambda_g \rho_g c_g}} > \tau \quad (6)$$

Fuels at any given thickness, therefore, can be expected to behave as thin fuels in a quiescent microgravity environment.

The energy balance of Eq. (3) should be adjusted for thin fuels, and must account for radiative losses, given the large residence times, $t_{res,g} = t_{res,s} \sim L_g / V_f$, possible in a quiescent environment. We include only solid reradiation in the energy balance to capture the radiative effects.

$$V_{f0} \rho_s c_s L_{sy} W (T_v - T_\infty) + \epsilon \sigma (T_v^4 - T_\infty^4) L_{gx} W \sim \lambda_g (T_f - T_v) W \quad (7)$$

$$\text{Or, } \eta_0 \equiv \frac{V_{f0}}{V_{f,Thin}} \sim \frac{1}{2} + \frac{1}{2} \sqrt{1 - 4\mathfrak{R}_0}, \quad \text{where, } \mathfrak{R}_0 = \frac{1}{F^2} \frac{\rho_g c_g}{\rho_s c_s} \frac{\epsilon \sigma \tau}{\lambda_g} \left(\frac{T_v^4 - T_\infty^4}{T_v - T_\infty} \right) \quad (8)$$

Equations (8) reveals several characteristics of flame spread in a completely quiescent environment. The radiative effects can be seen to reduce the spread rate from its thermal limit $V_{f,Thin}$, the severity depending on the parameter \mathfrak{R}_0 . The minimum spread rate is reached at $\mathfrak{R}_0 = 1/4$, when the spread rate becomes half its thermal limit. Any increase in \mathfrak{R}_0 beyond this critical value will produce an imaginary spread rate, indicating extinction. Equation (8) thus yields a critical fuel thickness above which steady spread cannot be sustained. There is no comprehensive data to validate this claim. However, the steady spread rate at quiescent-environment for thin cellulosic fuel[8] and extinction for thick PMMA[9] are qualitatively consistent with Eq. (8).

The MGLAB data[2] for spread over PMMA of three different thicknesses at several opposing velocities is reproduced in Table 1 and Fig. 3. The extinction reported in the table is accompanied by relatively high values of \mathfrak{R}_0 , qualitatively consistent with conclusion from Eq. (8). The reduction in spread rate from the 1-g to microgravity environment (see Table 1) lends further support to the prediction from Eq. (8) that the spread rate decreases by 50% before extinction. The gradual reduction in spread rate, seen in Fig. 1, as the opposing velocity is reduced can be predicted from the energy balance equation (Eq. 7) by substituting $L_{gx} \sim \alpha_g / V_g$ for $V_g \gg V_f$, L_{sy} from Eq. (2), and treating the radiative term small compared to the sensible heating term in Eq. (7).

$$\eta_{thin} \equiv \frac{V_f}{V_{f,Thin,Thermal}} \sim 1 - \mathfrak{R}, \quad \eta_{thick} \equiv \frac{V_f}{V_{f,Thick,Thermal}} \sim 1 - 2\mathfrak{R}, \quad \mathfrak{R} = \frac{1}{F} \frac{\epsilon \sigma}{\rho_g c_g V_g} \left(\frac{T_v^4 - T_\infty^4}{T_v - T_\infty} \right) \quad (9)$$

Thickness \ O ₂ level	15μm	50μm	125μm
21%	extinct 13.4	extinct 4.2	extinct 1.4
30%	18.6 28.3	4.1 10.0	extinct 3.2
50%	39.1 55.1	18.9 22.8	Unsteady 8.1

Table 1. Spread rates in mm/s over PMMA in quiescent microgravity (upper number) and normal gravity conditions. Total pressure is 1 atm. Extinction occurs at high value of \mathfrak{R}_0 .

Note that while Eq. (8) clearly establishes thickness as an important parameter in the quiescent environment, the two limits in Eq. (9) also lend support this conclusion that the higher the fuel thickness, the higher is the radiative effects. Data shown in Fig. 2 is quite consistent with this conclusion.

SYMBOLS:

- ~ Equality within a order of magnitude
- ≈ Approximately equal
- ≡ Definition

CONCLUSIONS: We present here a scale analysis and some recent data acquired in the MGLAB, Japan, to investigate the role played by fuel thickness in opposed-flow flame spread. The major conclusions, some yet to be validated through proposed experiments [10], are as follows. 1. The critical non-dimensional thickness at which transition between thin and thick fuels takes place is $T \approx 2$, where T depends on the fuel and environmental parameters according to Eq.(7). 2. In a quiescent microgravity environment all fuels are thin fuels. 3. Steady spread is impossible in a quiescent environment for fuels above a critical thickness. 4. In the presence of opposing flow, the radiative effect decreases according to Eq. (9), which indicates two different limits for thermally thin and thick fuels.

ACKNOWLEDGEMENT: We gratefully acknowledge the support of NASA, Glenn Research Center and Japan Space Forum, and our technical monitor from NASA, Dr. Sandra Olson.

REFERENCES:

[1] Wichman, I.S., Prog. Energy Combust. Sci., Vol. 18, pp. 646-651 (1992).

[2] Takahashi, S., Nagumo, T., Wakai, K., and Bhattacharjee, S., JSME Int. Journal, Series B, Vol. 43, No. 4., pp. 556-562, (2000).

[3] Williams, F.A., Sixteenth Symposium (International) on Combustion, The Combustion Institute, Pittsburgh, PA, p. 1281, (1976)

[4] Delichatsios, M.A., Twenty-Sixth Symposium (International) on Combustion, The Combustion Institute, Pittsburgh, PA, p. 1281, (1996).

[5] Bhattacharjee, S., West, J., and Altenkirch, R.A., Twenty-Sixth (International) Symposium on Combustion, pp. 1477-1485, The Combustion Institute (1996).

[6] de Ris, J.N., Twelfth Symposium (International) on Combustion, The Combustion Institute, Pittsburgh, PA, p. 241, (1969).

[7] Bhattacharjee, S., King, M., Takahashi, S., Nagumo, T., and Wakai, K., A., Twenty-Seventh (International) Symposium on Combustion, The Combustion Institute (2000)

[8] Bhattacharjee, S., and Altenkirch, R.A., Twenty-Fourth (International) Symposium on Combustion, Combustion Institute, Pittsburgh, PA, pp. 1669-1676, (1992).

[9] Altenkirch, R.A, Tang, L., Sacksteder, K., Bhattacharjee, S., and Delichatsios, M.,A., Twenty-Seventh (International) Symposium on Combustion, The Combustion Institute (1998)

[10] Bhattacharjee, S., Wakai, K., and Takahashi, S., *Dynamics of Flame Spread in Microgravity Environment*, Office of Space Science Applications, NASA , 2000-2003.

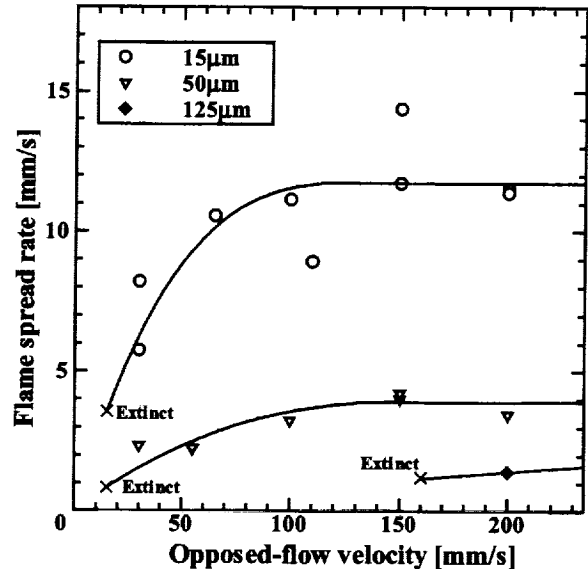


Fig. 3 Spread rate vs. opposed-flow velocity for PMMA in 21% O₂ and 1atm. (Data obtained in MGLAB, Japan)